Future Batteries 9 (2026) 100137

Contents lists available at ScienceDirect

Future Batteries

journal homepage: www.sciencedirect.com/journal/future-batteries

Derivation and experimental analysis of Peukert's equation in terms of fractional equivalent circuits☆

Michael J. Cree [a],*, Marcus T. Wilson [b], Jonathan B. Scott [a]

[a] School of Engineering, University of Waikato, Private Bag 3105, Hamilton, 3240, New Zealand
[b] School of Science, University of Waikato, Private Bag 3105, Hamilton, 3240, New Zealand

ARTICLE INFO

Dataset link: Peukert (Original data)

Keywords:
Battery
Peukert's equation
Fractional capacitance
Constant phase element
Equivalent circuit model
Riemann–Liouville integral

ABSTRACT

Using an equivalent circuit model (ECM) of a battery that involves fractional elements we analytically derive Peukert's empirical equation along with generalisations of the equation for the increasing capacity of the battery as the charge and discharge currents are reduced. The derived generalised Peukert's Equations are dimensionally consistent and all parameters (including Peukert's coefficient and the so-called 'capacity constant') can be calculated from the parameters of the ECM and operating voltage range of the battery. Experiments are conducted on ten batteries to demonstrate that the resistor fractional-capacitor series ECM fit to discharge times predicts well the impedance spectrum found by electrochemical impedance spectroscopy (EIS), and vice versa, on Li-CO/NCA/NMC and Na-ion batteries. This agreement is not observed on the tested $LiFePO_4$ and LiTO batteries because the impedance spectrum exhibits behaviour not captured by the ECM. Peukert's Equation predicts ever increasing capacity as *both* the charge and discharge currents are reduced. The experimental results confirm this behaviour for all batteries down to the lowest current measured (C/256).

Introduction

Peukert [1] first observed that the charge withdrawn from a fully charged lead–acid battery is dependent on the discharge current, with the charge withdrawn reduced at greater discharge currents. A similar relationship has also been observed for Li-ion battery cells [2–6]. Because estimating the useable charge remaining in a partially discharged battery with Coulomb counting is proving insufficiently reliable, there is some renewed interest in whether methods based on Peukert's Equation may prove to be more reliable [4–11].

Peukert's Equation states that for a discharge current I, the charge Q removed from a battery is given by

$$I^n Q = \text{const}, \tag{1}$$

for some battery specific constant on the RHS. Taking a constant current discharge, and discharge time t_d, the charge removed is given by,

$$Q = \int_0^{t_d} I\,dt = It_d. \tag{2}$$

Hence Peukert's Equation can be expressed as

$$I^k t_d = \text{const}, \tag{3}$$

where $k = n + 1$ and it is k that is known as the Peukert coefficient for the battery, and is typified by values of $1 \leq k \lessapprox 1.3$ for Li-ion batteries and up to 1.5 for lead–acid batteries.

Peukert's Equation is a phenomenological equation; there appears to be no known theoretical foundation for it other than qualitative explanations from aspects of battery electrochemistry. The equation is known to be true for only a limited range of currents, but these claims need careful qualification, particularly for very small currents. It would appear from Eq. (1) that in the limit of zero current infinite charge is removed, thus it is claimed that Peukert's equation must break down for sufficiently small currents [12] due to it being unphysical in the limit [2,9,13–16]. In many studies the charge current is fixed so that the battery always receives a charge of Q_c when charging, and if it is assumed that is the only charge available for discharge, then Peukert's Equation must eventually break down as the discharge current is reduced.

Empirical evidence for this breakdown of Peukert's Equation remained somewhat scarce until recently, and some cite the work of D'Alkaine et al. [17], but their Fig. 4 (for which the claim of violation of Peukert's Equation is made) consists of three data points over a very limited current range, which, in our opinion, is insufficient evidence

☆ This research did not receive any specific grant from funding agencies in the public, commercial, or not-for-profit sectors.
* Corresponding author.
E-mail addresses: michael.cree@waikato.ac.nz (M.J. Cree), marcus.wilson@waikato.ac.nz (M.T. Wilson), jonathan.scott@waikato.ac.nz (J.B. Scott).

https://doi.org/10.1016/j.fub.2025.100137
Received 29 September 2025; Received in revised form 11 December 2025; Accepted 28 December 2025
Available online 30 December 2025

to distinguish between Peukert's Equation and other potential relationships. Likewise, a similar claim of the low-current breakdown made by Galushkin et al. [2] for their Fig. 3 is obfuscated by the use of a linear scale and multiple data sequences plotted on the same graphs. Nevertheless, clear evidence of this expected breakdown can be found in recent literature [6,9,18].

One may argue that one should ensure that the battery is first fully charged when conducting an experiment to establish discharge capacity (hence the fixed charge current and charge capacity Q_c). But what is fully charged? Presumably Peukert's Equation applies not only to the discharge capacity but also to the charge capacity Q_c. If so, and the battery is charged at ever decreasing currents that are same as the following discharge current, then the charge capacity Q_c itself will increase in accordance with Peukert's Equation, and sufficient charge will always be available to the discharge so that Peukert's Equation can be obeyed even at extremely low currents. It would appear that under these conditions in the limit of zero current that infinite energy can be stored and then recovered during discharge! This possibility requires further investigation.

On the other end of the scale it is well known that for large currents, such as current draws that occur for short periods in electric vehicles, the loss of available capacity can be noticeably reduced beyond that predicted by Peukert's Equation. The most obvious explanation is that the voltage drop across the internal resistance for a sufficiently large discharge current will drop the battery voltage immediately to its minimum discharge voltage, thereby stopping discharge and resulting in zero charge removed [9,18]. In other words, assuming a minimum operating voltage and non-zero internal resistance, there is a maximum discharge current beyond which no charge can be removed.

There is no theoretically derived model from more fundamental principles to accurately characterise the shape of the curve as it deviates from Peukert's Equation to instant discharge at the maximum possible discharge current. Interestingly, there is some variation observable in the shapes of the curve for plots of either discharge capacity (Q) or discharge time (t_d) for high discharge currents that can be found in the literature [2,6,8,19]. Notable is Fig. 2 of Galushkin et al. [6], which shows two regimes in which different power laws are fit to the data before internal resistance takes over. Fig. 1 of Rudy et al. [19] also clearly shows similar behaviour for some of their Li based test cells. Other evidence might be inferred from the graphs of capacity provided by Nebl et al. [8] in which some cases roll-off more slowly at higher currents than what might be expected if internal resistance was solely in play. It would therefore be premature to exclude the possibility that there are factors other than the internal resistance in play at high currents.

A number of attempts have been made to modify Peukert's Equation to account for the high-current deviation from Peukert's prediction but they are all empirically derived equations chosen for their goodness of fit to experimental measurements. That is, they are essentially guesswork and there is no theoretical foundation to prefer one over another other than goodness of fit to experimental data. We do note one empirical model: the seemingly independent proposals by Nebl et al. [8] and Yazvinskaya et al. [9] of multiplying Peukert's Equation by the first-order linear low-pass filter equation. Both groups demonstrate that this equation fits experimental data well for their measured Li battery cells and supercapacitors. (It appears in their experiments that the internal resistance of the tested device was sufficiently small to have little effect at the currents tested.) What is not pointed out in these studies, but is significant, is that the filter equation that they used interpolates between two power laws, corroborating the evidence of Galushkin et al. [6] mentioned above. That two power laws seem to be in play at different current regimes, at least in some results presented in the literature, needs further investigation.

Criticism is sometimes made that Peukert's Equation is dimensionally inconsistent [3,20], thus cannot be truly physical [20]. Often the constant on the RHS of Peukert's Equation, Eq. (3), is taken to be the capacity of the battery at a standard discharge rate, thus is said to have units of charge (either C or Ah), which is not consistent with the units of the LHS which has fractional units if $k \neq 1$. In this paper we shall argue that Peukert's Equation is, in fact, dimensionally consistent, and that the constant on the RHS has been misidentified.

The studies cited are primarily focussed on developing a useful generalisation of Peukert's Equation that can be used in a battery management system. Theoretical explanations for Peukert's Equation and its generalisations are lacking. An insightful step towards doing this is provided by Mills and Kim who link Peukert's coefficient to a fractional capacitance in a supercapacitor that is revealed by electrochemical impedance spectroscopy (EIS) [21,22], however, there are clear limitations in their exposition: they treat fractional capacitance as a frequency dependent capacitance (which is to misunderstand it [23]), and the metrology presented is incapable of sufficiently characterising fractional behaviour of Li-ion batteries.

Though ignored by much of the literature, fractional behaviour has long been considered important for building realistic physical or equivalent electrical circuit models of battery cells. Considering diffusive processes at the electrode, Randles [24] first proposed an equivalent circuit model (ECM) involving a Warburg element (fractional capacitance of order 0.5). Westerhoff et al. [25] expanded the model for a typical Li battery cell to 16 electrical components including three fractional capacitors and two Warburg elements. It is not feasible to characterise all these elements with standard non-destructive measurement techniques in the presence of noise [26], nor is it clear that they are even needed for reliable circuit modelling of a battery cell. Using recently developed EIS methodology that can measure down to ultralow frequency (microhertz) [27,28], Poihipi et al. [29] showed that an ECM consisting of a resistor and one or two fractional capacitors (also known as constant phase elements or CPE) in series, which we call the R-cpe and R-cpe-cpe models, is sufficient to model the frequency dependent impedance up to approximately 1 Hz of many types of Li-ion batteries.

Further evidence that these simple fractional ECMs can capture much of the complex behaviour of Li-ion batteries comes from fundamental considerations of the electrochemistry. Recent considerations of restricted diffusive processes through porous electrodes [30,31] lead to an impedance model that behaves as a Warburg element in the high frequency limit and as an ideal capacitor in the low frequency limit. The R-cpe-cpe model naturally captures this behaviour if the primary CPE has order 1 (an ideal capacitor being the primary energy storage element of the battery) and the secondary CPE has order 0.5 (the Warburg element). At frequencies above about 1 Hz the charge-transfer process and double layer capacitance become significant [32], but for our purposes play an insignificant role and can be omitted from the model as studies on Peukert's Equation primarily exercise frequencies much lower than 1 Hz. Finally, we note that the R-cpe and R-cpe-cpe models have been demonstrated to produce results amongst the best for time-domain simulation of lithium ion battery cell voltage [33].

In this paper we analytically derive Peukert's law and its generalisations from a simple battery cell ECM involving fractional capacitance thereby giving a theoretical foundation to Peukert's Equation. We show that Peukert's coefficient is related to the order of the fractional capacitor and give an expression for the constant on the RHS that is dimensionally consistent with the fractional units of the LHS. We revisit the very low current limit and show that due to the fractional nature of the ECM, it is possible to devise an experimental procedure with which behaviour in accordance with Peukert's Equation is observed down to very low currents that are much lower than reported before. We explain the deviations from Peukert's Equation at high current due to the internal resistance and suggest how the presence of a second CPE in the ECM could lead to the detectable presence of a secondary power law. We back this up by comparison to experimental data and show how one can estimate the parameters of the model via the resultant generalised Peukert's Equation from data obtained when cycling the battery with various discharge currents.

Theory

In this section we more formally introduce fractional capacitance and describe the ECM of a battery that includes a CPE. From this ECM we derive a generalisation of Peukert's Equation that under certain experimental conditions and the limit of zero internal resistance reduces exactly to Peukert's Equation. The derivation gives an explicit formula for the constant on the RHS of Peukert's Equation and shows that it is dimensionally consistent. We conclude the theory section with simulated 'measured' data points from the model and show that the model can be reliably fit to the data giving back the parameters of the ECM.

Fractional capacitance

A fractional capacitor, or constant phase element (CPE), exhibits an admittance spectrum with a fractional order α, $0 < \alpha < 1$, and a constant phase between the voltage and current of $-\alpha\pi/2$ radians or $-\alpha \times 90°$. The special case of $\alpha = 1$ is a pure capacitor, while $\alpha = 0$ is a resistor. Their behaviour can be defined through fractional calculus. Generally, the current and voltage follow the relationship:

$$I(t) = C_F \frac{d^\alpha V(t)}{dt^\alpha}, \tag{4}$$

where the right-hand-side involves a *fractional derivative*. In this work it is more useful to consider how voltage $V(t)$ depends on current $I(t)$, and we can invert this relationship through a Riemann–Liouville (RL) differintegral, specifically (for $0 < \alpha < 1$):

$$V(t) = \frac{1}{C_F \Gamma(\alpha)} \int_\tau^t I(t')(t-t')^{\alpha-1}\, dt' \tag{5}$$

where $\Gamma(\cdot)$ is the gamma function and τ is a starting point in the past. One notable feature is that the fractional-derivative is not local in time—the element has memory of its past [23,34].

The impedance of a fractional capacitor expressed as a function of frequency in the Laplace form follows naturally from Eq. (4):

$$Z_{CPE} = \frac{1}{C_F (j\omega)^\alpha} \tag{6}$$

where $j^2 = -1$. Note, it is only in the limit $\tau \to -\infty$ (i.e. when all history is considered) that the complex exponentials are eigenfunctions of the RL differintegral (Eq. (5)), hence that RL is consistent with Eq. (6) [35].

Fractional battery model

Poihipi et al. [29] showed that the R-cpe and R-cpe-cpe ECMs (see Fig. 1) can be reliably fit to the impedance spectrum of Li-ion batteries in the presence of noise, provided that the EIS is performed to ultralow frequencies (i.e. well into the microhertz range). The R-cpe ECM of a battery, Fig. 1(a), consists of a resistance R_s in series with a CPE of capacity C_F and order α. The R-cpe-cpe model, Fig. 1(b), consists of a series resistance R_s, a primary CPE (C_1, α_1) in which most of the energy storage occurs, and a secondary CPE (C_2, α_2). The R-cpe-cpe model often gives a small but useful improvement of the fit to the impedance spectrum over the R-cpe model particularly in the 0.1–5 mHz range. Also shown in Fig. 1 is the R-cpe-Zarc model in which a Zarc element, which here consists of a Warburg element (a CPE with $\alpha = 0.5$) in parallel with a resistor, replaces the secondary CPE. We find this model, which was not considered by Poihipi et al., is needed to fit the impedance spectrum well on $LiFePO_4$ and LiTO batteries. It is important to realise that these circuits constitute the complete model of the battery—there is no non-physical ideal voltage source modelling the open circuit voltage (OCV) of the battery in the ECM.

In the following derivations we focus on the R-cpe model as it is easier to manipulate analytically. In principle, the behaviour of the battery depends on its entire history, thus is intractable to calculate. Instead, we consider the battery to have been charged to some positive voltage in the past, which has decayed to an open circuit voltage of V_l at time $t = 0$, and that over the duration of the experiment it further decays by an amount smaller than the resolution of measurement, thus V_l can be taken to be constant.

Charging the CPE with a constant current I_0 from time t_1 to time t_2 by evaluation of the Riemann–Liouville differintegral gives the voltage $V_c(t)$ of the CPE at any time t as [33],

$$V_c(t) = \frac{I_0}{C_F \Gamma(\alpha+1)} \left[(t-t_1)^\alpha H(t-t_1) - (t-t_2)^\alpha H(t-t_2)\right], \tag{7}$$

where $H(\cdot)$ is the standard Heaviside (or unit-step) function and $\Gamma(\cdot)$ is the gamma function. The voltage $V_b(t)$ of the battery during the charge cycle with current I_0 from $t = 0$ to time t, using the R-cpe ECM and the above assumption about the battery's past, is therefore given by

$$V_b(t) = V_l + I_0 R_s + \frac{I_0}{C_F \Gamma(\alpha+1)} t^\alpha. \tag{8}$$

Peukert's equation with R-cpe model

To derive Peukert's Equation we continue to use the R-cpe ECM of a battery cell. We take the simplified case of charging the battery with current I_c to voltage V_h from time 0 to time t_c then discharging at a possibly different current $I_d = \lambda I_c$ for time t_d until the battery reaches the minimum voltage V_l. We do not include a constant-voltage (CV) charging phase (as normally included in practice) to simplify the analysis. Eq. (8) gives the voltage during charging, and on setting $V_b(t_c) = V_h$ for the end of charging and rearranging, gives the time to charge as,

$$t_c = \left[(V_h - V_l - I_c R_s)\frac{C_F \Gamma(\alpha+1)}{I_c}\right]^{1/\alpha}. \tag{9}$$

Now during discharge, $t_c < t \le t_c + t_d$, the CPE voltage is given by

$$V_c(t) = V_l + \frac{I_c}{C_F \Gamma(\alpha+1)}\left[t^\alpha - (t-t_c)^\alpha\right] + \frac{-I_d}{C_F \Gamma(\alpha+1)}(t-t_c)^\alpha \tag{10}$$

$$= V_l + \frac{1}{C_F \Gamma(\alpha+1)}\left[I_c t^\alpha - (I_c + I_d)(t-t_c)^\alpha\right], \tag{11}$$

which at the end of discharge becomes $V_c(t_c + t_d) = V_l + I_d R_s$, hence

$$V_l + I_d R_s = V_l + \frac{1}{C_F \Gamma(\alpha+1)}\left[I_c (t_c+t_d)^\alpha - (I_c + I_d) t_d^\alpha\right], \tag{12}$$

or,

$$R_s C_F \Gamma(\alpha+1) = \frac{I_c (t_c+t_d)^\alpha - (I_c+I_d) t_d^\alpha}{I_d}, \tag{13}$$

$$= \frac{(t_c+t_d)^\alpha - (1+\lambda) t_d^\alpha}{\lambda}. \tag{14}$$

If the series resistance $R_s = 0$ then

$$t_d = \frac{t_c}{(1+\lambda)^{1/\alpha} - 1}. \tag{15}$$

Multiplying both sides by I_d gives the discharge capacity Q_d as,

$$Q_d = \frac{\lambda Q_c}{(1+\lambda)^{1/\alpha} - 1}, \tag{16}$$

where Q_c is the charge capacity.

Note that for a CPE that is a capacitor ($\alpha = 1$) the charge recovered during discharge is equal to the charge given during charge, and the discharge time is in proportion to the charge time by the ratio λ of discharge and charge currents. For the CPE that is a resistor ($\alpha = 0$) the discharge time is zero (i.e., all charge is lost whatever the value of λ). For a CPE that is a fractional capacitor ($0 < \alpha < 1$) the discharge time is always such that the discharge capacity is less than the charge capacity, namely $Q_d < Q_c$ for all $\lambda \ge 0$ and $0 \le \alpha < 1$, as given by Eq. (16). Hence, in a fractional system, some charge is lost between charge and discharge. (Interestingly, some of that lost charge can be recovered by resting the battery for a while then resuming the discharge, but we do not explore that possibility any further here.)

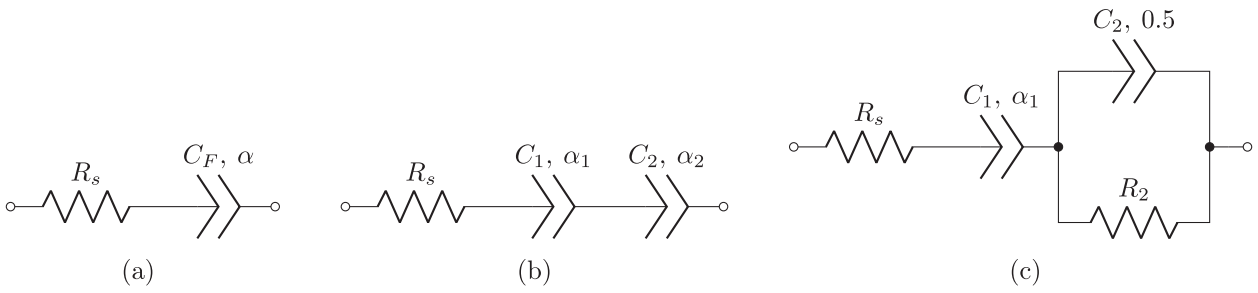

Fig. 1. Equivalent circuit models of the battery (a) R-cpe model (b) R-cpe-cpe model. (c) R-cpe-Zarc model where the CPE in the Zarc is taken to be a Warburg element (i.e., α is fixed to be 0.5).

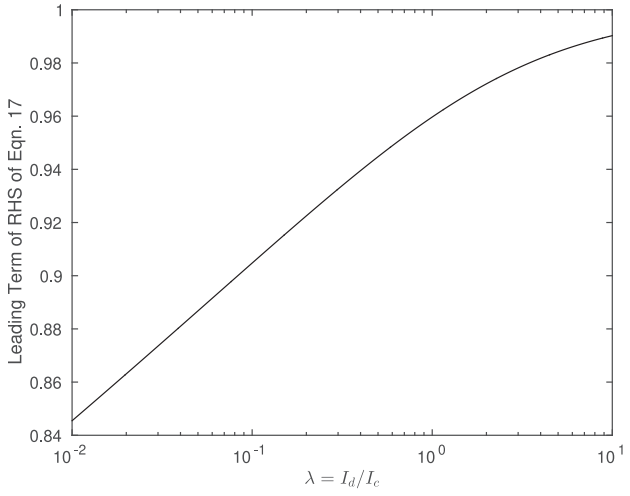

Fig. 2. The term $\lambda^{1/\alpha}/[(1+\lambda)^{1/\alpha}-1]$ of Eq. (17) for $\alpha = 1/1.03$.

Substituting for t_c from Eq. (9) in Eq. (15) (still with $R_s = 0$) and rearranging, gives

$$I_d^{1/\alpha} t_d = \frac{\lambda^{1/\alpha}}{[(1+\lambda)^{1/\alpha}-1]} \left[(V_h - V_l)\, C_F \Gamma(\alpha+1)\right]^{1/\alpha}, \tag{17}$$

which has the appearance of Peukert's Equation (Eq. (3)) if we take Peukert's coefficient to be $k = 1/\alpha$, the inverse of the fractional capacitor order, excepting that there is an additional leading term in λ rendering the RHS non-constant in general. Nevertheless, this expression has two advantages over Peukert's Equation as normally expressed, namely (1) the equation is dimensionally consistent (note that the units of C_F are $\mathrm{A\,s^{\alpha}V^{-1}}$ or equivalently $\mathrm{F\,s^{(\alpha-1)}}$) and (2) the constant on the RHS (i.e. ignoring the term in λ) is expressed in terms of ECM parameters and the operating voltage range.

Fig. 2 shows the leading term in λ of Eq. (17) for a Peukert's coefficient of $k = 1.03$ ($\alpha \simeq 0.97$) typical for a Li-ion battery. For λ in the range of 0.1 to 10, there is less than $\pm 6\%$ variation in this term, hence for discharge currents from 1/10-th of up to 10 times the charge current there is little deviation from Peukert's Equation. As the discharge current is further reduced below 1/10-th, the discharge time is noticeably reduced below that predicted by Peukert's Equation.

Two different experimental procedures

Now consider two different experimental procedures. The first is the commonly practised procedure for I_c to be fixed and unchanging. In these experiments only the discharge current is reduced for each subsequent charge/discharge cycle. The limit of zero discharge current ($\lambda \to 0$), obtainable by application of L'Hôpital's rule to Eq. (16), gives the maximum total charge obtained during discharge as

$$\lim_{\lambda \to 0} Q_d = \alpha Q_c, \tag{18}$$

where Q_c is a fixed value. Hence, for a fractional system ($\alpha < 1$) the charge recovered during discharge is always less than that given during charging and reaches the value αQ_c when discharge current is reduced to zero. The discharge time and current satisfies Eq. (17) with $\lambda = I_d/I_c$.

The second experimental procedure is for identical charge and discharge currents reduced in lockstep on each subsequent cycle, that is, $\lambda = 1$ always. Then

$$Q_d = \frac{Q_c}{2^{1/\alpha}-1}. \tag{19}$$

Substituting $Q_c = I_c t_c = I_d t_c$ with t_c given by Eq. (9) with $R_s = 0$, gives

$$Q_d = \frac{[(V_h - V_l) C_F \Gamma(\alpha+1)]^{1/\alpha}}{2^{1/\alpha}-1} I_d^{1-1/\alpha}. \tag{20}$$

hence as the discharge current is reduced the capacity increases, without limit, in a power law relationship. Note that this increase disappears for a true capacitor ($\alpha = 1$). Finally, note that evaluating Eq. (17) for $\lambda = 1$, results in,

$$I_d^{1/\alpha} t_d = \frac{\left[(V_h - V_l)\, C_F \Gamma(\alpha+1)\right]^{1/\alpha}}{2^{1/\alpha}-1}, \tag{21}$$

which is indeed Peukert's Equation (with $k = 1/\alpha$). The RHS is now a constant that can be evaluated from parameters of the model and the cycling voltage limits.

Let us now consider a non-zero internal resistance R_s. Analytical solution of Eq. (13) for t_d is not straightforward, but the equation can be inverted numerically to give t_d with a reasonable initial guess and a few iterations of the Newton–Raphson method. To better understand the equation let us consider the limit of very small current. The time to charge t_c (Eq. (9)) is essentially the same as the case of zero internal resistance (because $I_0 R_s \ll V_h - V_l$), likewise for the time to discharge because as t_c gets large, the constant term due to R_S on the LHS becomes relatively smaller, thus t_d is given by Eq. (15) in the limit of zero current. Thus, even with non-zero internal resistance, we would expect in the limit that either discharge capacity is limited to αQ_c or that Peukert's Equation is obeyed, depending on which of the two experimental procedures is undertaken.

For sufficiently large current, the argument given in the Introduction applies: the voltage drop across the internal resistance becomes so large to terminate charging immediately thus there is a maximum charge current, $I_{\mathrm{max,c}} = (V_h - V_l)/R_s$, for which $t_c = 0$. A similar expression can be found for the maximum discharge current by setting $t_d = 0$ in Eq. (13) to get,

$$I_{\mathrm{max,d}} = \left(\frac{\lambda}{\lambda+1}\right) I_{\mathrm{max,c}} = I_{\mathrm{max,c}} - I_c. \tag{22}$$

The middle equality is the most useful for evaluating $I_{\mathrm{max,d}}$ for experiments with fixed $\lambda = 1$ giving $I_{\mathrm{max,d}} = I_{\mathrm{max,c}}/2$. For experiments where the charge current I_c is fixed, the right-most expression is the most convenient for calculating $I_{\mathrm{max,d}}$.

To highlight the difference between the two experimental procedures we plot in Fig. 3 the discharge time and capacity for two systems:

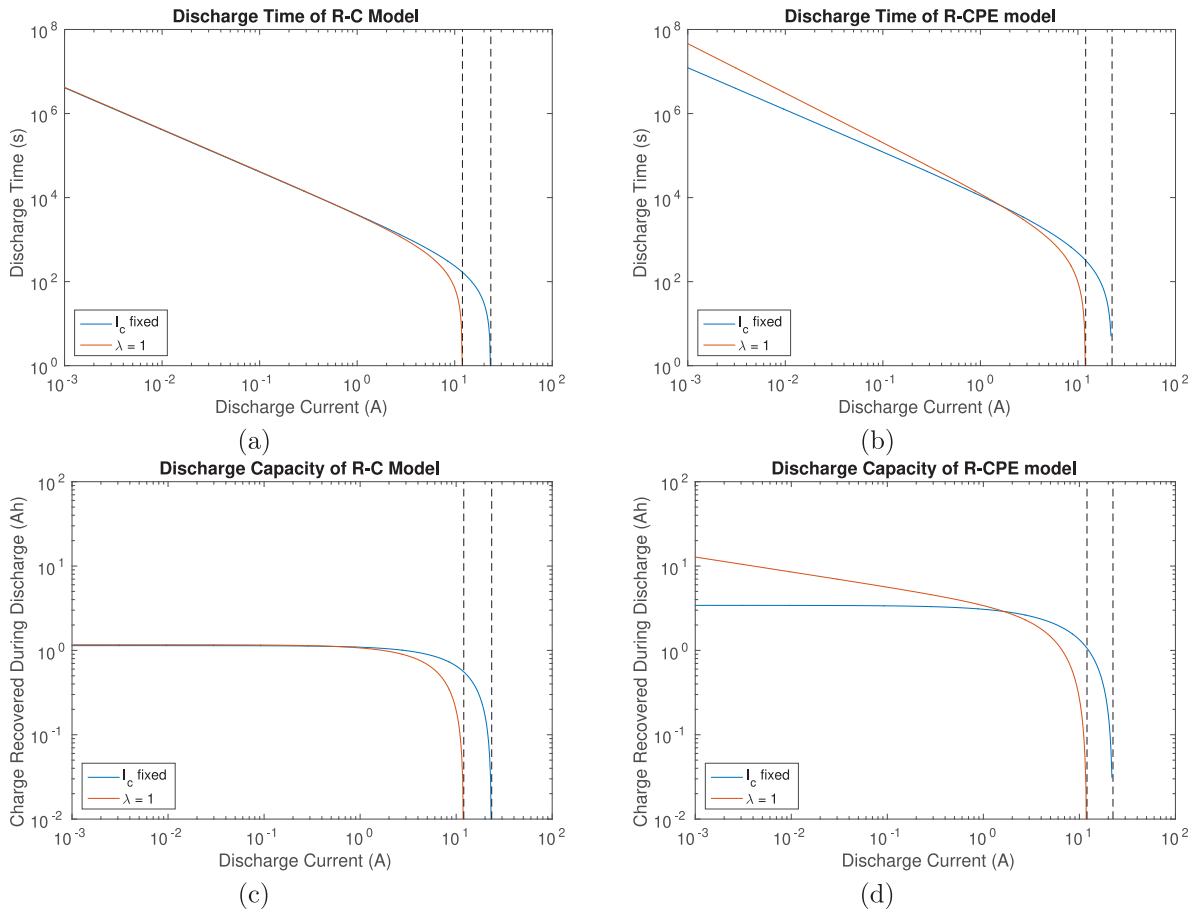

Fig. 3. Discharge time and capacity of the R-C and R-CPE models. Left column RC model ($\alpha = 1$); Right column: R-CPE model ($\alpha = 0.85$); Top row: discharge time; Bottom row: discharge capacity. The vertical dashed lines indicate the asymptote due to internal resistance.

a resistor–capacitor series (R-C) circuit model and a resistor-CPE series (R-CPE) circuit model. We take values that are representative of a Li-ion (NMC) 18650 cell, namely $R_s = 50\ m\Omega$ and $C_F = 3500\ F\,s^{\alpha-1}$, with $\alpha = 1$ to give the R-C model and $\alpha = 0.85$ to give the R-CPE model (a value smaller than might be expected of an 18650 cell chosen here to emphasise the difference for illustration purposes). For the R-C circuit model (Fig. 3 left column) there is no difference between the two experimental procedures at lower currents when the voltage drop across the internal resistance is insignificant, likewise the discharge capacity is limited and unchanging in the low-current regime as would be expected for an ideal capacitor.

The fractional system however shows notably different behaviour dependent on the experimental procedure (Fig. 3 right column). If the charge current is fixed then charge withdrawn is limited to that given during charging as is the case for the R-C model. However, if the charging current is reduced in lockstep with the discharge current the discharge capacity increases according to Peukert's Equation (indeed, Eq. (21)). This result suggests an experiment to expose fractional behaviour in a battery which we exploit in the experiments reported below. Finally, we caution the reader not to make too much of the increased capacity of the R-CPE model over the R-C model in Fig. 3. The units of fractional capacitance C_f are not the same between the two models thus the capacity cannot be directly compared.

To further examine the R-cpe system we plot in Fig. 4, the charge and discharge times versus current, along with the zero resistance asymptote (Eq. (17)) and predicted maximum currents in dashed red lines. This is for the experimental procedure in which $\lambda = 1$, that is, $I_d = I_c$. Firstly, we stress again the capacity continues to increase as current is reduced as expected from Peukert's Equation. A bizarre mathematical implication of fractional calculus is that a CPE can store, in principle, infinite energy at a finite voltage. This apparent paradox is resolved by understanding that a CPE needs infinite time to store this energy. Secondly, note at low currents when the effect of the series resistance is insignificant, that the discharge capacity is *always* less than the charge capacity by a fixed proportion, indeed to that given by Eq. (19).

Simulated fitting of model

With the model above for the dependence of time to charge and/or discharge against current one can make measurements on a battery of the charge or discharge times for various currents and then fit the models to numerically infer the model parameters. We demonstrate that here for simulated measurements, using the R-CPE model, with plots presented in Fig. 4.

We select a current from C/64 up 4C for the battery cell from each octave and generate the time to charge/discharge from the R-cpe model. We add Gaussian noise to each selected point, being 1 mA standard-deviation for the current and 1 s standard-deviation for the time, and then quantise to the nearest 1 mA for current and 1 s for time, to simulate the measurement process.

We fit times to charge ($t_{c,i}$) to the (simulated) measured currents ($I_{0,i}$) using Eq. (9) to find the model parameters for the R-cpe model using the Matlab nlinfit function. To have a good chance of convergence it is necessary to fit the model in log–log space. (An alternative is to minimise squared relative error instead of squared absolute error.) It is also necessary to detect bad values of the model parameters as Matlab searches the parameter space for the solution and take appropriate action to avoid non-finite function results so the search

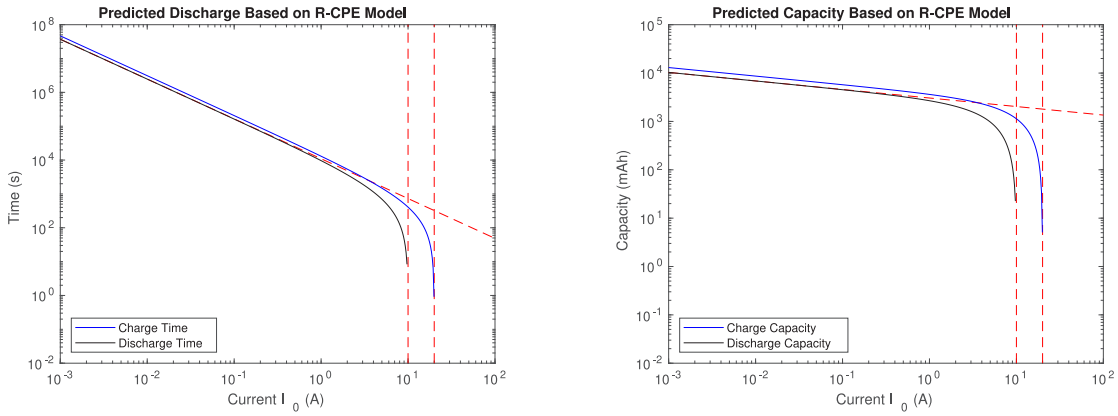

Fig. 4. Predicted charge/discharge time (left) and capacity (right) for a typical 18650 Li-ion cell using the R-cpe equivalent circuit model. The dashed red lines are the low-current asymptote and the maximum possible currents for charge and discharge.

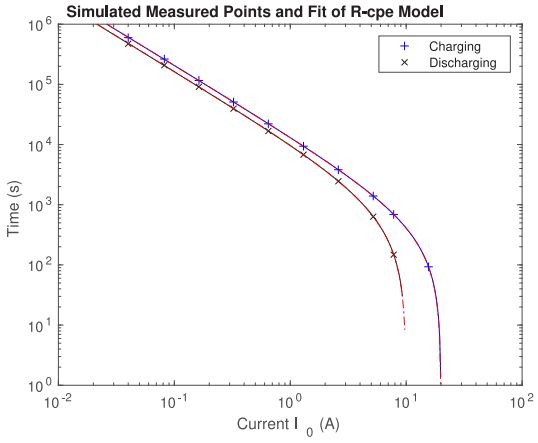

Fig. 5. Fit of R-cpe model to simulated measured points on the charge and discharge curves. Measured points as per legend. Solid black/blue lines are the fitted curves to the two sets of data points. Overlaid red dashed curves is the original model generating the data points.

Table 1
R-cpe example model parameters and fitted parameters to simulated measured data points.

	R_s (Ω)	C_F ($F\,s^{\alpha-1}$)	α	RMSE
Model	0.0500	3500	0.850	
Charge-fit	0.0499	3510	0.850	0.0075
Discharge-fit	0.0500	3480	0.849	0.0077

for the solution can continue. The result is plotted in Fig. 5 with the found model parameters listed in Table 1. We also fit Eq. (13) to the measured discharge times. The result is also plotted in Fig. 5 with found model parameters listed in Table 1. The fits to currents and times of charge/discharge gave very similar results essentially identical to the known model parameters.

These results demonstrate that we can fit to data points measured over three decades of current, provided that current measurements are made in the regime where the internal resistance is having an appreciable effect. We note that this is not a demonstration one can fit the ECM to actual data measured from a battery. To that end let us now turn our attention.

Table 2
Batteries used in experiments. NCA is nickel–cobalt–aluminium, NMC is nickel–manganese–cobalt.

Label	Part-Num	Chemistry	Capacity	V_h	V_l	Currents
UBCO-X	INR18650-MJ1	Li-NMC	3.4 Ah	4.2 V	2.8 V	0.05–6.8 A
UBCO-Y	INR18650-MJ1	Li-NMC	3.4 Ah	4.2 V	2.8 V	0.05–6.8 A
S30Q-1	INR18650-30Q	Li-NMC	3.0 Ah	4.2 V	3.0 V	0.0117–4.24 A
PBD-1	NCR18650BD	Li-NCA	3.0 Ah	4.2 V	3.0 V	0.0117–1.50 A
S26J-1	ICR18650-26JM	Li-CoO	2.6 Ah	4.2 V	3.0 V	0.0102–0.65 A
NA-1	NA-32140	Na-ion	10 Ah	3.95 V	2.0 V	0.039–5.00 A
IFR1	IFR18650-E1600	$LiFePO_4$	1.6 Ah	3.5 V	3.0 V	0.0063–1.60 A
IFR2	IFR18650-E1600	$LiFePO_4$	1.6 Ah	3.5 V	3.0 V	0.0063–0.566 A
IFR26-1	IFR26650-38A	$LiFePO_4$	3.8 Ah	3.5 V	3.0 V	0.0148–5.37 A
LTO-drive	66160H 40Ah	LiTO	40 Ah	2.5 V	2.0 V	0.156–12 A

Experimental methodology

We cycled (charge and discharge) ten batteries (see Table 2) at various currents over the range C/64 to 2C (UBCO batteries) and C/256 to the currents listed in Table 2 (all others), and measured the charge and discharged times. Most batteries were pre-used to some extent, either in an electric bike (UBCO) or in laboratory experimentation (most others). Only the battery NA-1 was newly purchased. The voltage range used for cycling is narrower than that specified by manufacturers for normal operation to avoid the substantial change in incremental capacity that can occur near full discharge or charge. Experimentation was conducted with a Chroma Battery Tester (17216M-6-12) that was controlled by custom software run on a Raspberry-PI. Experiments were carried out in an air-conditioned room with temperature held between 21 °C and 23 °C (with one short excursion to 25 °C).

All batteries had been rested for some time (>1 month) before experimentation began, except for NA-1 (25 days) and the two UBCO batteries (6 days). At each tested current the batteries were first charged to V_h at constant current (CC) and rested for 600 s. Cycling then began consisting first of a discharge at the same current (CC) to V_l, resting for four hours, then charging to V_h at CC, then resting for 600 s. The discharge/charge cycle was performed two-times at the lower currents (C/256 to C/32) and three-times at the higher currents (C/16 and above). When cycling at a current had completed, the battery was rested for a day before starting cycling at the next current. The UBCO batteries were cycled at the highest currents first, then the current was reduced for each subsequent cycling experiment. All other batteries were cycled at the lowest current first and then the current was increased for each subsequent cycling experiment. For analysis the discharge times were taken from the second cycle only for those experiments that had two cycles and from the mean of the second and third cycle for those experiments that had three cycles. This procedure

Table 3
Parameters of models fit to the UBCO-X battery data.

Model	R_s (mΩ)	C_1 ($F s^{\alpha_1-1}$)	α_1	C_2 ($F s^{\alpha_2-1}$)	α_2	R_2 (mΩ)	RMSE
EIS R-cpe	74.2	4937	0.917	–	–	–	0.075
EIS R-cpe-cpe	66.3	10 903	1.002	194	0.282	–	0.017
EIS R-cpe-Zarc	68.5	8313	0.976	340	0.500	33.0	0.009
DT R-cpe	69.8 (3.8)	6588 (999)	0.973 (0.017)	–	–	–	0.011

ensures all reported discharge times are preceded by a charge of the same current as required by the $\lambda = 1$ experimental procedure.

An EIS was also performed on the batteries covering the frequency range starting at 5 or 10 μ Hz up to 2 or 5 Hz. R-cpe, R-cpe-cpe and R-cpe-Zarc model fits were performed in frequency space to the EIS data by methods described elsewhere [28,29]. We use the parameters found from the discharge times (DT) R-cpe model fit to predict the impedance spectrum and likewise the parameters found from the EIS R-cpe model fit to impedance data to predict discharge times, notwithstanding the limitations of such comparisons (see Discussion below).

Results

The results fall into two classes: those (the first six batteries listed in Table 2, namely all batteries except the $LiFePO_4$ and LiTO batteries) that have reasonable agreement of the R-cpe model transfer from discharge times to EIS and vice versa and those ($LiFePO_4$ and LiTO batteries) where there is no agreement in the R-cpe model transfer from discharge times to EIS and vice versa because the R-cpe model fails to describe the impedance spectrum well. In this section we show results for the two UBCO batteries and S30Q-1 as examples of the first class and IFR26-1 as an example of the second class. Results for all other batteries can be found in the supplementary material.

The EIS performed on the UBCO-X battery with accompanying R-cpe and R-cpe-Zarc model fits are presented in Fig. 6. The parameters of the fitted models are listed in Table 3 with 95% confidence intervals on parameters in parentheses for the discharge times model fit. The measured discharge times are plotted in Fig. 6(c) with a fit of the R-cpe model to the discharge times (using Eq. (13) with t_c given by Eq. (9)), and with the resultant R-CPE model fit to the discharge times used to plot the impedance in Fig. 6(d).

The R-cpe model fits to discharge times of the UBCO-Y, S30Q-1 and IFR26-1 batteries are shown in Fig. 7 on the measured discharged time (left column) and used to predict the EIS (right column). The parameters found in the model fitting are listed in Table 4 (UBCO-Y), Table 5 (S30Q-1) and Table 6 (IFR26-1). The fitted R-cpe parameters from discharge times and EIS on the UBCO-Y and S30Q-1 batteries (likewise for PBD-1, S26J-1 and NA-1 in the Supplement) can be used to make a reasonable prediction of the other. Notably for these batteries the found CPE fractional order α_1 from the discharge times agrees reasonably well with that found for the primary CPE (α_1) in the EIS R-cpe-Zarc model fit. Two comments are needed: (1) The S30Q-1 battery is less successful in that the DT R-cpe fit over estimated the series resistance, probably because measured currents are insufficiently high to reliably expose the effect of the series resistance. (2) The agreement of the primary CPE order of battery PBD-1 (see Table 7 and the Supplement) is not as good as the other batteries.

In the case of the IFR26-1 battery the measured EIS spectrum is not well represented by the R-CPE model (Fig. 7 bottom row), nevertheless clear, well-fitted, R-CPE behaviour is seen when fitting the discharge times. The two R-CPE models (from the discharge times and EIS) fail to predict the other. The R-cpe-Zarc model fits the IFR26-1 impedance spectrum far better than the other simpler models (see Supplement) indicating that $LiFePO_4$ batteries exhibit more complex behaviour than Li-NCA/NMC batteries. The LiTO battery (LTO-drive in the Supplement) exhibits similar problematic behaviour due to the failure to fit the R-cpe model to the impedance spectrum.

Incremental capacity

The prediction of incrementing capacity for decreasing current for the $\lambda = 1$ experimental procedure is tested in Fig. 8 in which the measured discharge capacities for six of the batteries cycled down to a current of C/256 are plotted on a log–log scale. Two curves are shown in the graphs: the first (Q CPE model) is a linear regression to discharge capacities of the first four currents (C/256, C/128, C/64 and C/32), in effect, a fit of the CPE model in the limit of low current where the internal resistance should have no effect. The second curve (DT R-CPE Model) is the capacity predicted using the R-cpe model fit to the discharge times of the section above.

All batteries (except arguably LTO-drive) demonstrate increasing capacity as current of cycling is reduced. In Table 7 the found fractional order from the capacity Q CPE model and the DT R-CPE model, along with the primary CPE order of the EIS R-cpe-Zarc model are listed for comparison. For the first four batteries there is good agreement, but for the last two where the R-cpe model does not fit the impedance spectrum well, there is poor agreement between the discharge time and capacity model fits and the primary CPE of the impedance R-cpe-Zarc model.

For the IFR26-1 battery the DT R-CPE model calculated at all available currents fails to predict the discharge capacities, indeed it has found a fractional order greater than one for the CPE, which is, of course, nonsense. If the DT R-CPE model fit is restricted to discharge times for currents up to C/1.4 only then a superior DT R-CPE model fit is obtained (see dashed line of the IFR26-1 graph of Fig. 8). This model fit reasonably predicts the discharge times of the highest two currents (that were not used in the fit) but is also underestimating the CPE order, thus undercuts the capacity measurements at the lowest two currents.

Discussion

We have analytically derived a generalised Peukert's equation from an R-cpe fractional series ECM for batteries. Cycling experiments to measure the times-to-discharge performed on nine Li-ion batteries and one Na-ion battery show that the R-cpe model can fit the experimental data well. The derived parameters of the R-cpe model from discharge times used to predict the impedance fit the experimental measured EIS reasonably well for the Li-NCA, Li-NMC, Li-CO and NA-ion batteries. Likewise the R-cpe model parameters derived from the EIS impedance spectrum used to predict the discharge times of cycling also fit the measured data well for these batteries. It was not successful for the $LiFePO_4$ and LiTO batteries because the measured impedance spectrum exhibits complicated behaviour not captured by the R-cpe model.

The goodness of fit when transferring from time-domain to frequency-domain and vice versa is especially encouraging for two reasons. The first is that the RL differintegral used to derive the generalised R-cpe Peukert equation has been criticised for not being formally consistent with the one-sided Laplace frequency description [35]. The inconsistency is due to the need to include all history (and can be reformulated as an initial condition problem [36]) which we managed by making a reasonable assumption about the pre-history of the battery. That the presented cycling experiments did not exactly meet the assumed history of the battery cell seems not to be a problem.

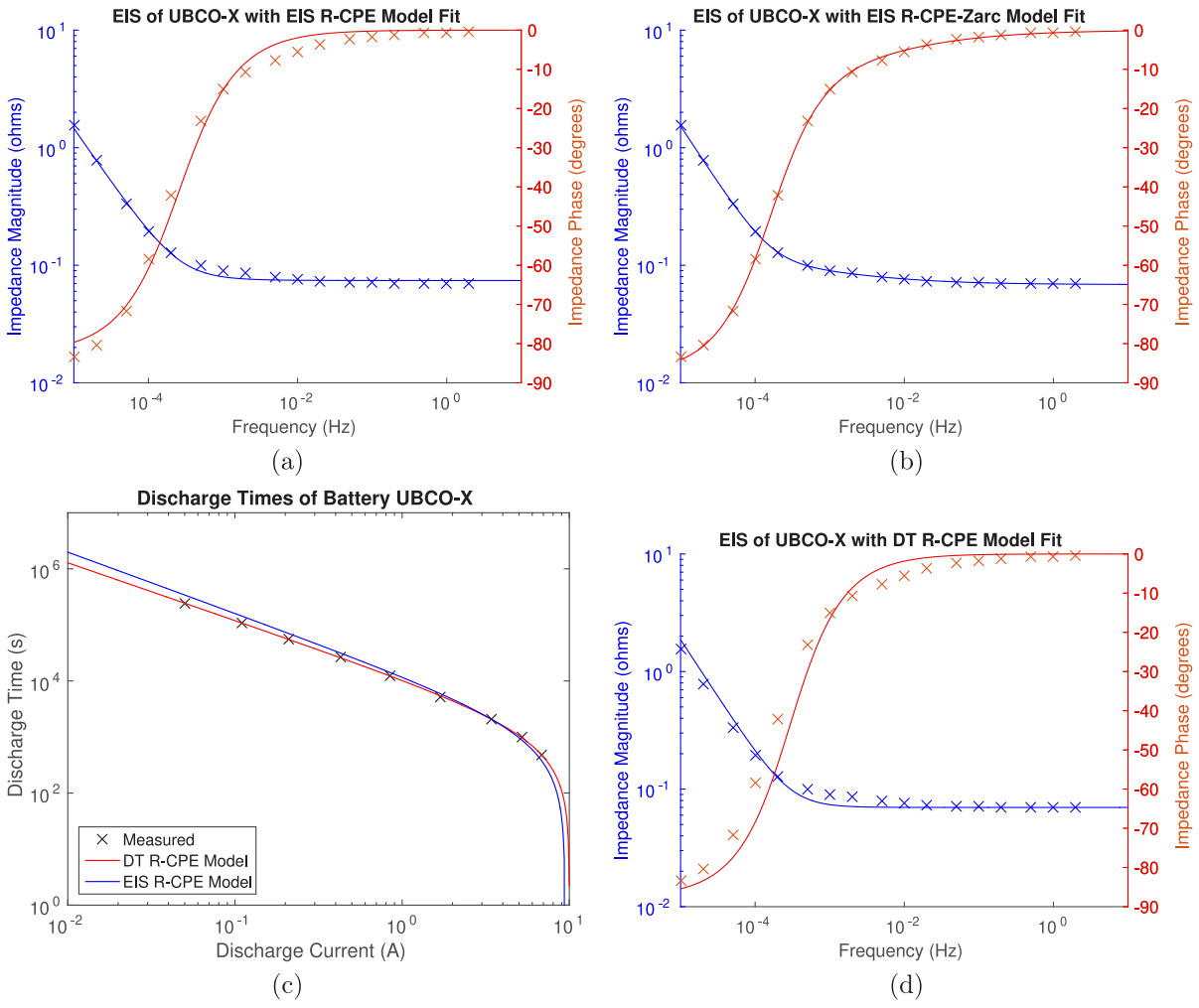

Fig. 6. Model fit to EIS and discharge times (DT) of the UBCO-X battery. (a) R-cpe model fit to EIS. (b) R-cpe-Zarc model fit to EIS. (c) Discharge times with overlaid R-cpe model fits to discharge times and EIS. (d) R-cpe model from discharge times overlaid measured EIS.

Table 4
Parameters of models fit to the UBCO-Y battery data.

Model	R_s (mΩ)	C_1 ($F s^{\alpha_1-1}$)	α_1	C_2 ($F s^{\alpha_2-1}$)	α_2	R_2 (mΩ)	RMSE
EIS R-cpe	74.8	4915	0.916	–	–	–	0.073
EIS R-cpe-cpe	67.0	10 597	0.998	195	0.279	–	0.017
EIS R-cpe-Zarc	69.2	8118	0.973	340	0.500	31.9	0.009
DT R-cpe	74.1 (3.6)	6933 (1081)	0.979 (0.018)	–	–	–	0.012

Table 5
Parameters of models fit to the S30Q-1 battery data.

Model	R_s (mΩ)	C_1 ($F s^{\alpha_1-1}$)	α_1	C_2 ($F s^{\alpha_2-1}$)	α_2	R_2 (mΩ)	RMSE
EIS R-CPE	27.3	4044	0.900				0.152
EIS R-CPE-CPE	21.4	11 870	1.014	210	0.305		0.038
EIS R-CPE-Zarc	23.0	8334	0.981	305	0.500	32.3	0.021
DT R-CPE	44.9 (5.2)	7797 (593)	0.993 (0.008)				0.006

Table 6
Parameters of models fit to the IFR26-1 battery data.

Model	R_s (mΩ)	C_1 ($F s^{\alpha_1-1}$)	α_1	C_2 ($F s^{\alpha_2-1}$)	α_2	R_2 (mΩ)	RMSE
EIS R-CPE	21.7	131	0.397				0.056
EIS R-CPE-CPE	Failed to fit						
EIS R-CPE-Zarc	23.6	4395	0.717	186	0.500	180	0.021
DT R-CPE	41.3 (1.4)	36 166 (8971)	1.041 (0.028)				0.011

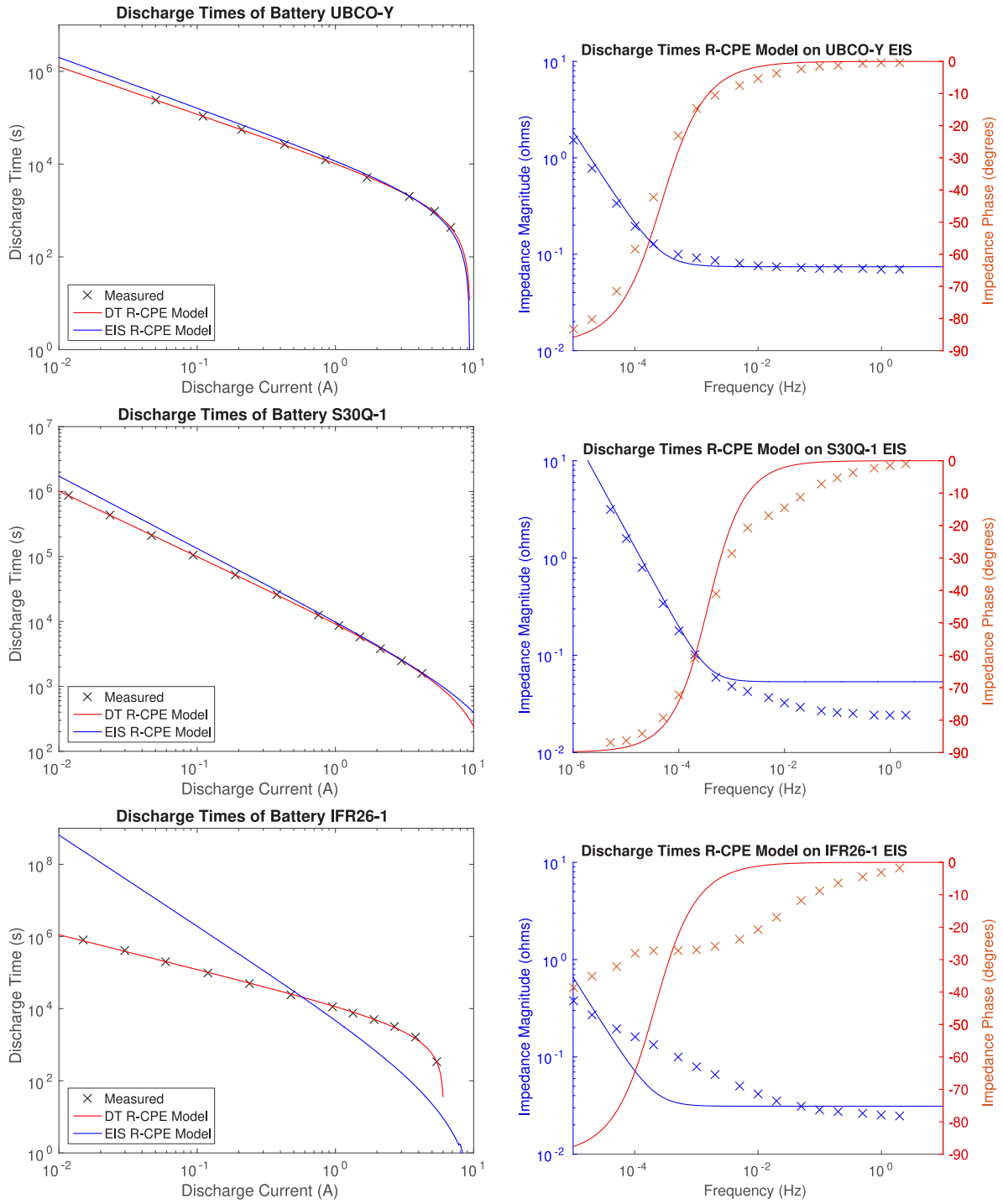

Fig. 7. Discharge times (DT) R-cpe model fitted to the UBCO-Y, S30Q-1 and IFR26-1 batteries. Left column: discharge time fit (red) to measured data points with the curve predicted by the EIS determined model overlaid (blue). Right column: EIS measured data overlaid with the prediction by the discharge time R-CPE model fit.

The second reason is that the EIS is based on a linear small-signal model and is conducted within a localised SoC of the battery cell. The fact that cycling experiments reveal regions of different incremental capacity at different states of charge within batteries is suggestive that the R-cpe model parameters should be a function of SoC thus any model parameters derived from an EIS will depend (to some extent) on what SoC the EIS was performed at. In contrast, fitting to the time to discharge in Peukert type cycling experiments is performed over the whole voltage range which includes regions of non-linear behaviour, the most notable of which is the collapse of incremental capacity of a battery cell at lower voltages.

In our experiments the used voltage ranges were tighter than manufacturers' specifications (see Table 2) to avoid the non-linear regions that occur for many battery chemistries below approximately 20% SoC and above 90% SoC. In contrast, the UBCO batteries were cycled between 2.8 to 4.2 V which includes the fall-off in incremental capacity

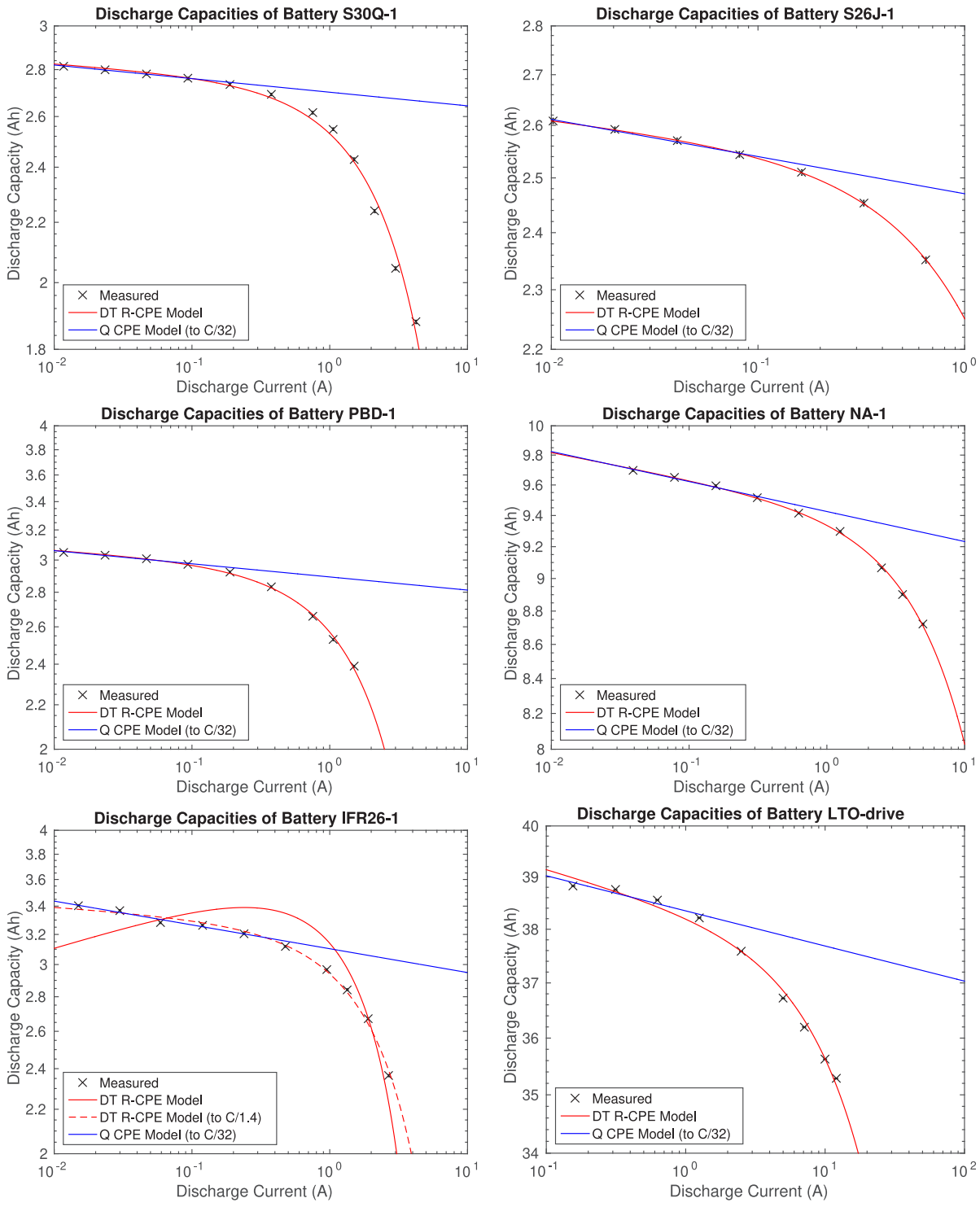

Fig. 8. Discharge capacities of various batteries at very low currents (down to C/256).

Table 7
Primary CPE order (α) of fit to discharge capacities (parentheses are the 95% CI in the last digits).

Battery	S30Q-1	S26J-1	PBD-1	NA-1	IFR26-1	LTO-drive
Q CPE Model	0.991 (2)	0.988 (3)	0.988 (5)	0.991 (3)	0.978 (17)	0.992 (7)
DT R-CPE Model	0.993 (8)	0.992 (1)	0.991 (4)	0.992 (1)	1.041 (28)	0.991 (–)
EIS R-CPE-Zarc Model	0.981	0.969	0.942	0.989	0.717	0.884

below 3.2 V. Nevertheless good agreement with the R-cpe Peukert model was obtained, possibly because the incremental capacity falls so much that the time to traverse this region is quite small compared to the time spent in the linear region, thus has a negligible impact on the final result.

The R-cpe fit to discharge times (see Tables 3 to 5, and the Supplement) found internal resistance values either very close (UBCO-X and UBCO-Y) or a bit bigger (S30Q-1, PBD-1, S26J-1) to the EIS R-cpe fit for the Li-ion batteries, but CPE values (particularly regards the fractional order of the CPE) much closer to that of the primary CPE of the EIS R-cpe-Zarc fit. To explain this behaviour, note that the current stimulus for cycling and measuring discharge times is very close to a square-wave stimulus. As the current is reduced the frequency of the charge and discharge cycle decreases proportionally (more precisely in accordance with the generalised Peukert's model) so, in essence, point-by-point impedance spectroscopy contaminated by harmonics of the stimulus is performed by a Peukert-like experiment (particularly true for the $\lambda = 1$ experimental procedure used herein). Our experiments had discharge times of up to 10^6 seconds, that is, a stimulus fundamental frequency of 1 μ Hz, which is well into the region where the primary capacitor-like CPE is dominant on the EIS graphs (see Figs. 6 and 7 and the Supplement). Hence the Peukert cycling experiment is dominated by the primary CPE of the R-cpe-Zarc model in the low current regime. Further note that the resistance is largely in effect from 1 mHz on the UBCO batteries' EIS but not clearly into effect until 10 mHz or higher on the S30Q-1, PBD-1, S226-1 EIS (see Supplement), but out experiments rarely got above 1C current, which is a cycling frequency of 0.13 mHz, and at this frequency the impedance has not decreased to that of the internal resistance for these batteries, hence the inflated resistance values for the DT R-CPE model fit.

This observation can also help explain why the fractional order found by the DT R-cpe model fit on the $LiFePO_4$ batteries (IFR1, IFR2 and IFR26-1) does not agree with the fractional order of any ECM model fits to the EIS (see Tables 6 to 7 and the Supplement). It is clear from the EIS spectra (particularly from the phase) for these batteries (see Fig. 7 and the Supplement) that even at 5 μ Hz (the lowest frequency measured) that near capacitor-like CPE behaviour is not seen, and one might guess that the EIS would need to be measured down to even lower frequency to expose such behaviour. The DT R-cpe model fits suggest this is true, as the asymptotic discharge capacity behaviour that is close to an ideal capacitor (see Fig. 8 and Supplement) is clearly evident at the lowest currents (C/256 up to C/32) which have cycling fundamental frequencies of 0.5 μ Hz up to 4 μ Hz, which are all below the lowest frequency in the EIS graphs.

In the literature on Peukert's Equation [6,8,19] there is (admittedly circumstantial) evidence of a second power law (i.e. CPE) sometimes present in the discharge time graphs. The presence of a second CPE has been identified in measured EIS data [29] and observable herein for the EISes presented in Figs. 6 and 7 (and the Supplement). One can develop a generalised R-cpe-cpe Peukert Model involving two CPEs to calculate the voltage across the battery at the end of charge ($t = t_c$) and discharge ($t = t_c + t_d$). For $\lambda = 1$, thus $I = I_c = I_c$, the result is,

$$V_b(t_c) = V_h = V_l + I\left(R_s + \frac{t_c^{\alpha_1}}{C_1\Gamma(\alpha_1)} + \frac{t_c^{\alpha_2}}{C_2\Gamma(\alpha_2)}\right), \tag{23}$$

and

$$V_b(t_c + t_d) = V_l = V_{;} - I\left(R_s + \frac{2t_d^{\alpha_1} - (t_c + t_d)^{\alpha_1}}{C_1\Gamma(\alpha_1 + 1)} + \frac{2t_d^{\alpha_2} - (t_c + t_d)^{\alpha_2}}{C_2\Gamma(\alpha_2 + 1)}\right), \tag{24}$$

however inverting these for t_c and t_d is not analytically tractable. They can be solved numerically, however we found that numerical fitting of the R-cpe-cpe model to our measurements of times to charge and discharge for the UBCO batteries (which had measurements to the highest currents) was incapable of distinguishing between the secondary CPE and the internal resistance. We thus could not find evidence for the second CPE in discharge times despite its presence is quite clearly seen in the EIS data for the same batteries. The difficulty of distinguishing a secondary CPE from the internal resistance has been noted before for fitting a fractional series ECM to time domain data that reflects normal battery usage [33,37]. It is possible, however, that with better sampling of high-current measurements the model might have successfully converged in our experiments and revealed the second CPE. Further experimentation is required to examine this possibility.

We noted earlier (Section "Peukert's Equation with R-cpe Model") that a CPE can, in principle, store infinite energy, exactly in agreement with Peukert's Equation, provided the correct experimental procedure is undertaken. On a discharge capacity versus current graph that would be seen as a continued increase in capacity of the battery as the charge and discharge currents are reduced. Scant evidence contrary to this surprising conclusion can be found in the literature, mostly because reported studies undertake an experimental procedure that is incapable of revealing this behaviour. In our experiments we got down to C/256 current for many of the tested batteries. We see no clear deviation from Peukert's Equation on any of the batteries at such low currents.

Of course, these experiments are no proof that Peukert's Equation would not eventually break down as the current is reduced even further. The troubles with conducting such experiments is the prohibitive length of time to perform them and the limit on resolution in measuring very small currents. We note, finally, that we do expect Peukert's Equation to ultimately break down at sufficiently low currents (despite the mathematical prediction of fractional calculus) because the ECM is a macro-description of the battery that is only valid in the limit of extremely many electrons involved in the current flow. At very low currents we would expect other effects such as thermal currents to become significant.

Conclusion

Using fractional calculus we derived Peukert's Equation and generalisations of Peukert's Equation from a series ECM involving fractional components. The R-cpe model was shown to fit experimental discharge times measured on ten batteries well, and was further confirmed by then correctly predicting the impedance against measured EIS data on six of those batteries. In the other direction, the R-cpe model fit from the EIS predicted the discharge times well for the same six batteries. This cross-fitting between discharge times and the EIS on the remaining four batteries (the $LiFePO_4$ and LiTO batteries) failed because the EIS spectrum exhibited complicated behaviour not well modelled by R-cpe. Fitting of the more general R-cpe-cpe model was unsuccessful because the discharge times measured in the conducted experiments provided insufficient data to distinguish a secondary CPE from the internal resistance of the series ECM.

The generalised Peukert's Equations presented herein have the advantages that they are dimensionally consistent and that the constant, rather than being arbitrarily assigned a capacity at some discharge rate, is instead expressed in terms of parameters of the model and the voltage range the battery is operated over. Furthermore the fractional order of the CPE of the model is shown to be the inverse of the Peukert's coefficient of the battery.

A prediction of fractional calculus (and of Peukert's Equation) is that the capacity increases for decreasing discharge currents and eventually can become infinite for an infinitely long charge time with infinitesimal current, provided that the battery is charged at the same current that it is subsequently discharged at. Our tests down to C/256 confirmed this predicted behaviour.

CRediT authorship contribution statement

Michael J. Cree: Writing – review & editing, Writing – original draft, Visualization, Software, Project administration, Methodology, Investigation, Formal analysis, Data curation, Conceptualization. **Marcus T. Wilson:** Writing – review & editing, Methodology, Investigation, Conceptualization. **Jonathan B. Scott:** Writing – review & editing, Methodology, Investigation, Conceptualization.

Declaration of competing interest

The authors declare that they have no known competing financial interests or personal relationships that could have appeared to influence the work reported in this paper.

Acknowledgements

We are grateful for the insightful comments from an anonymous reviewer that enabled us to substantially improve the paper during revision.

Supplementary data

Supplementary material related to this article can be found online at https://doi.org/10.1016/j.fub.2025.100137.

Data availability

Research Link Provided

Peukert (Original data) (Gitlab)

References

[1] W. Peukert, Electronisch. Z. 20 (1897).
[2] N.E. Galushkin, N.N. Yazvinskaya, D.N. Galushkin, Appl. Sci. 10 (2020) 5518.
[3] Q. Zhang, N. Cui, Z. Zhou, Y. Shang, B. Duan, Int. J. Ener. Res. 46 (2022) 23808–23823.
[4] D. Doerffel, S.A. Sharkh, J. Pow. Sourc. 155 (2006) 395–400.
[5] N. Omar, P. van den Bossche, T. Coosemans, J. van Mierlo, Energy 6 (2013) 5625–5641.
[6] N.E. Galushkin, N.N. Yazvinskaya, D.N. Galushkin, J. Electrochem. Soc. 167 (2020) 120516.
[7] Y.-H. Sun, H.-L. Jou, J.-C. Wu, 2008 IEEE International Conference on Sustainable Energy Technologies (ICSET2008), Singapore, 2008, pp. 101–105.
[8] C. Nebl, F. Steger, H.-G. Schweiger, Int. J. Electrochem. Sci. 12 (2017) 4940–4957.
[9] N.N. Yazvinskaya, N.E. Galushkin, D.N. Galushkin, A.V. Alepko, Int. J. Electrochem. Sci. 14 (2019) 7973–7982.
[10] F. Steger, J. Krogh, L. Meegahapola, H.-G. Schweiger, Energy 15 (2022) 7902.
[11] J. Xie, J. Ma, K. Bai, J. Pow. Electron. 18 (3) (2018) 910–922.
[12] M. Cugnet, M. Dubarry, B.Y. Liaw, ECS Trans. 25 (35) (2010) 223–233.
[13] N. Galushkin, N. Yazvinskaya, D. Galushkin, Int. J. Electrochem. Sci. 9 (2014) 1911–1919.
[14] N.E. Galushkin, N.N. Yazvinskaya, D.N. Galushkin, J. Electrochem. Soc. 162 (3) (2015) A308–A314.
[15] N.E. Galushkin, N.N. Yazvinskaya, D.N. Galushkin, Int. J. Electrochem. Sci. 14 (2019) 2874–2882.
[16] N.N. Yazvinskaya, N.E. Galushkin, D.V. Ruslyakov, D.N. Galushkin, Processes 9 (2021) 1753.
[17] C.V. D'Alkaine, A. Carubelli, H.W. Fava, A.C. Sanhueza, J. Pow. Sourc. 53 (1995) 282–292.
[18] N.N. Yazvinskaya, M.S. Lipkin, N.E. Galushkin, D.N. Galushkin, Energy 15 (2022) 2825.
[19] A.S. Rudy, A.M. Skundin, A.A. Mironenko, V.V. Naumov, Batteries 9 (2023) 370.
[20] L.A. Vicari, V.A. de Lima, A.S. de Moraes, M.C. Lopes, Orbital: Electron. J. Chem. 13 (5) (2021) 392–398.
[21] E.M. Mills, S. Kim, J. Phys. Chem. Lett. 7 (2016) 5101–5104.
[22] E.M. Mills, S. Kim, J. Electrochem. Soc. 167 (2020) 130506.
[23] S. Westerlund, L. Ekstam, IEEE Trans. Dielect. Elect. Insul. 1 (5) (1994) 826–839.
[24] J.E.B. Randles, Discuss. Faraday Soc. 1 (1947) 11–19.
[25] U. Westerhoff, K. Kurbach, F. Lienesch, M. Kurrat, En. Technol. 4 (2016) 1620–1630.
[26] F. Berthier, J.-P. Diard, R. Michel, J. Electroanal. Chem. 510 (2001) 1–11.
[27] J. Scott, R. Hasan, IEEE Access 7 (2019) 106925–106930.
[28] C. Dunn, J. Scott, IEEE Trans. Instrum. Meas. 71 (2022) 8003808.
[29] E. Poihipi, J. Scott, C. Dunn, J. Electroanal. Chem. 911 (2022) 116201.
[30] J.-D. Gabano, T. Poinot, B. Huard, Commun. Nonlinear Sci. Numer. Simul. 47 (2017) 164–177.
[31] H.-C. Yu, S.B. Adler, S.A. Barnett, K. Thornton, Electrochemica Acta 354 (2020) 136534.
[32] M. Zabara, G. Katırcı, F.E. Civan, A. Yürüm, S.A. Gürsel, B. Ülgüt, Electrochemica Acta 485 (2024) 144080.
[33] V. Farrow, J.B. Scott, M.J. Cree, M. Wilson, IEEE Access 12 (2024) 64589–64598.
[34] M.T. Wilson, L.I. Cowie, M.J. Cree, IEEE Access 13 (2025) 198289–198300.
[35] M.D. Ortigueira, V. Martynyuk, V. Kosenkov, A.G. Batista, Frac. Fractional 7 (2023) 86.
[36] M.D. Ortigueira, Mathematics 10 (2022) 1771.
[37] M.T. Wilson, V. Farrow, C.J. Dunn, L. Cowie, M.J. Cree, J. Bjerkan, A. Stefanovska, J.B. Scott, J. Phys. En. 7 (2025) 025001.